Numerical studies of floor heave control by the rock bolts reinforcement technology in retained gob-side gateroad

Ivan Sakhno[1,2*], *Svitlana* Sakhno[1,2], *Viacheslav* Kamenets[2], and *Edgar Caceres* Cabana[3]

[1]Donetsk National Technical University, 29 Sofii Kovalevskoi St., 43012 Lutsk, Ukraine
[2]LLC "Technical University "Metinvest Polytechnic", 80 Pivdenne Shose, 69008 Zaporizhzhia, Ukraine
[3]Universidad Nacional de San Agustin de Arequipa, Institute of Renewable Energy Research and Energy Efficiency, 107 San Agustin St., PE-04000 Arequipa, Peru

Abstract. The effectiveness of modified rock bolts reinforcement technology for floor heave control in gob-side entry retaining was studied in this paper. A finite-element numerical simulation was used to analyse stress-strain state of surrounding rocks before and after immediate floor reinforcement with six floor support schemes. It was found that after immediate floor reinforcement with rock bolts with diameter 32 mm and 96 mm, floor heave in retained gob-side gateroad reduces by 2.94 – 3.6 times respectively. The modification of rock bolt reinforcement scheme by the additional installation of piles in the entry corners was proposed. Piles installation significantly reduces the zone of horizontal and vertical post-peak strains in the gateroad floor. The best variant among compared ones is a floor support scheme with two corner piles, 1 m and 2 m long. With this scheme, floor heave decreases by 3.05 times. The comparison of the materials costs of the floor support schemes were performed. As a result, the most effective floor support scheme was proposed and prospects for the further progress of floor reinforcing technologies were outlined.

1 Introduction

The large deformations of surrounding rocks have become a major challenge for mining influenced roadways of deep coal mines. Actual repairing rate of underground roadways in Ukrainian mines is as high as 80% [1]. Similar repairing rate is noted by researchers from other countries [2, 3]. Significant part of these roadway repairs is caused by uncontrolled floor heave.

The floor heave control of mining roadways has always been the focus of geotechnical engineering researchers. In recent years, the pillarless mining technology has been increasingly used [4 – 6]. Floor heave mechanism in retained gob-side roadways has differences. Therefore, many studies have been conducted to study the floor heave mechanism and control technology of gob-side entry retaining [7, 8].

* Corresponding author: ivan.sakhno@donntu.edu.ua

Previous studies have indicated three main mechanisms of floor heave in underground coal mine: bearing capacity failure, swelling, and buckling [10 – 12]. However, different geological conditions and roadway support technologies lead to combination of the mechanisms described above. Thus, the combined effect of several mechanisms complicates the real floor heave process. This causes difficulties with choosing the optimal floor heave control method [13, 14]. Rock-mass classification systems have been developed to systematize the results of monitoring of the roadway deformation and generalize practical experience in roadway stability control in different geological conditions. These systems became a reliable methodology to follow in the pre-design stage of tunneling and mining [15]. For floor rock of coal mine Mo et al. [12] proposed rock mass classification known as CMFR system (Coal Mine Floor Rating). Components of the CMFR are uniaxial compressive strength and discontinuity spacing. Horizontal Stress Rating (HSR) and the Floor Heave Index were proposed [12]. In recent years these characteristics are the most widely used.

Moisture content has a significant influence on the floor uplift when the clay-rich materials are in the rock structure [16, 17]. The swelling mechanism of floor heave may appear at high moisture content [18, 19]. Moisture content can also be an additional complicating factor. Mentioned before and scholars [20, 21] studied the influence of water content on floor heave. However, in this paper this factor is not considered.

Most scientists represent the floor heave mechanism in gob-side entry retaining as capacity failure or buckling [22]. In both cases stress concentration is the key factor of floor heave [23]. Reinforcement and stress relief technologies were mainly proposed to floor heave control [24, 25].

Xie et al. [26] studied the effectiveness of stress relief technology in roadway under the mining dynamic pressure. The technical parameters of pressure relief during borehole-making were finally determined because of comparison of different schemes. T. Yang and J. Zhang [27] presented the numerical simulation results of stress distribution in the surrounding rock of the mine roadway under different slot depths. The effective parameters of the pressure-relief slot were determined. Guo et al. [28] discussed the control mechanism of floor rock burst with depressurization and support of roadway. In this method large diameter stress relief borehole, that was drilled in immediate floor, combined with pile was proposed. Li et al. [29] proposed the floor heave control technology based on combining the pressure relief of floor blasting and roof cutting. The stress relief methods are not widely used due to technical difficulty and expensiveness.

Reinforcement methods are the most popular ones. These methods are mainly focused on floor rock bolts, cable bolt, grouting reinforcement, and their combination. Lai et al. [30], put forward optimized rock bolt support scheme because of numerical simulation. He et al. [31] discussed floor heave control with bolt-net-anchor coupling support technology. Its effectiveness confirmed by the micro-fabric test, theoretic analysis, numerical simulation, and in-situ test. Yang et al. [32] proposed and applied in the field new coupling floor support technology of a bolt-mesh-anchor-base angle bolt-flexible layer truss. The numerical analysis and field monitoring was used to study the mentioned method. Shimada et al. [33], developed the cement grouting for floor reinforcement and cement-based grouting material that were studied by injection experiments and theoretical analysis. Zhang and Shimada [34] proposed grouting reinforcement to control the entry floor, and the corresponding effectiveness was verified by improving the rock mechanics of the floor strata. Sakhno et al. [16] studied inverted arch grouting reinforcement. It was found that the growth of the elasticity modulus of rocks in the grouted zone leads to a non-linear decrease of a floor heave. In the result of numerical simulation analysis, the prediction method of the floor heave magnitude for moisturized grouting reinforced rocks was proposed. Zhai et al. [35] proposed the combined supporting technology with bolt-grouting and floor pressure-

relief that effectively controls the surrounding rock stability of the deep head chamber at Xinzhuang coal mine.

Thus, the main element of most current reinforcement methods is rock bolt. Analysis of numerical simulation and in-situ monitoring shows that in the immediate floor of gob-side entry retaining rock bolts are bend, which reduces the reinforcement effect [36, 37]. In such conditions, replacement of bolts with piles has sometimes been recommended. Kang et al. [36] showed that the floor pile with floor grouting can effectively control the deformation of roadway floor. Xu et al. [38] proposed new steel pile method to control floor heave in gob-side entry retaining. Guo et al. [28] proposed floor heave control method with floor corner concrete-filled steel tube pile combined with grouting floor.

Summing up, despite significant progress in the development of floor heave control methods, floor restoration is often used in practice. Therefore, improving of floor heave control methods in gob-side entry retaining is actual problem of coal mining.

In this paper, floor heave mechanism and effectiveness of floor uplift control by the rock bolts reinforcement in gob-side retained gateroad of deep coal mine were studied. The stress-strain characteristics of surrounding rocks and support system were analyzed with finite-element method. The previous papers researching the effectiveness of rock bolts and floor pile methods have been mainly focused on their separate implementation. Piles were considered as a means of anti-slide effect, and rock bolts as a means of counteracting to rock stratification. Combining of these technologies has not been studied. The impact of rock bolt diameter on their effectiveness has not been studied. The main novelty of this paper is the study of effectiveness of floor heave control schemes with different rock bolts diameter and bolts-piles combination. As a result, the most effective floor heave control scheme was determined.

2 Engineering background

In this study, typical conditions for the Ukrainian Donbas were taken as an engineering background. C_{11} coal seam of Surgaia coal mine was the prototype. The thickness of seam is 1.4 m; the average inclination angle is 7º. The current depth of the mining is 900 m. The strata histogram and characteristic of roof and floor are shown in Fig. 1a.

a

Column	Lithology	Thickness (m)	Uniaxial strength of intact rock σ_c, (MPa)
	sandy mudstone	19.8	σ_c=44 MPa
	sandy mudstone	8.5	σ_c=37 MPa
	coal seam	1.4	σ_c=12 MPa
	mudstone	6.0	σ_c=31 MPa
	sandstone	24.0	σ_c=59 MPa

b

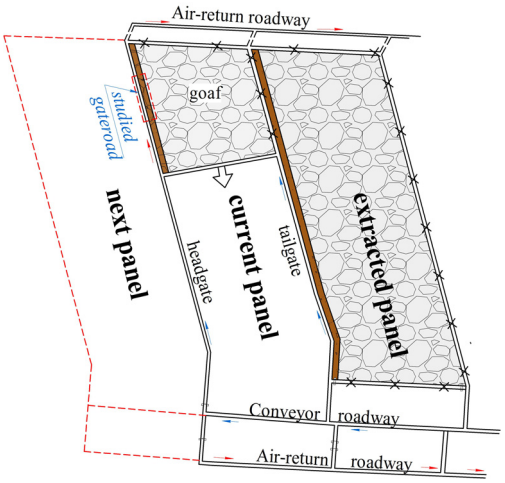

Fig. 1. Strata histogram (a), the roadway layout system (b).

Schematic diagram of pillarless method with the pointing of location of the studied gateroad is shown in Fig. 1b. The conveyor gateroad, which is supported behind the longwall face in the zone of established abutment pressure, was studied. A filling wall of Tekblend cement was used to support the roof behind the longwall face. Y-type ventilation scheme was applied. The prototype of the gateroad was the conveyor roadway of 14th eastern panel c11 coal seam. The gateroad was supported with U-shaped steel arches KSHPU-17.7 type from SVP-33 profile. The width and height of gateroad were 5.5 m and 4.2 m respectively. The steel arch frames spacing was 0.65 m. The gateroad view behind the longwall is shown in Fig. 2a, scheme of rupture shown in Fig. 2b.

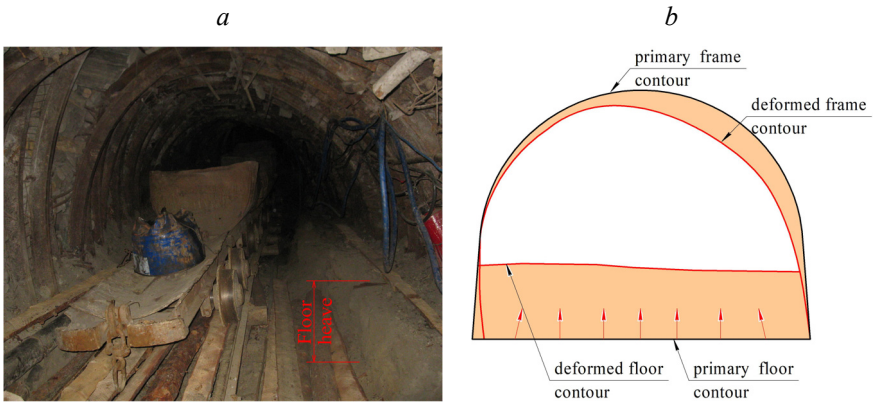

Fig. 2. The characteristics of rupture of retained gob-side gateroad: (a) the failure of U-shaped steel arch and the floor heave; (b) the characteristic of roadway failures.

The gateroad deformed asymmetrically (Fig. 2b). The steel arches were bend and deformed. The failure of the steel arch support was observed in the yielding nodes. The main stability problem was a large floor heave. The average vertical floor uplift in gob-side entry retaining was 1.15 m. Floor restoration with EL-160 Hazemag machine was used. Thus, can be concluded that the main restricting factor for the implementation of the pillarless method is dramatic floor heave.

3 Numerical model

The numerical simulation with finite element method by means of ANSYS software was performed. The Drucker-Prager model was used to simulate the behavior of rock mass and filling wall material. The adequacy of this approach to simulation the behavior of the heterogeneous rock mass and concrete material is shown in previous research [39, 40].To simulate the behavior of falled roof in goaf, the deformation modulus 30 MPa, and Poisson's ratio 0.45 were applied [41].

Numerical model was established according to the actual geological strata (Fig. 1a). The model was 1 m long, 60 m wide and 60 m high. Immediate floor had layered structure. Horizontal displacements were fixed at the respective lateral boundaries. Vertical displacements of model were fixed at the bottom boundary. The top boundary was set free. A vertical pressure of 22.5 MPa was applied on the top of the model. This pressure was equivalent to the strata weight at the depth of 900 m. The vertical gravity was set to 9.81 m/s^2.

A 5.5 x 4.2 m arch shaped roadway was modelled. Steel arch was simulated with beam element. The width of filling wall was 2.0 m. Numerical model is presented in Fig. 3.

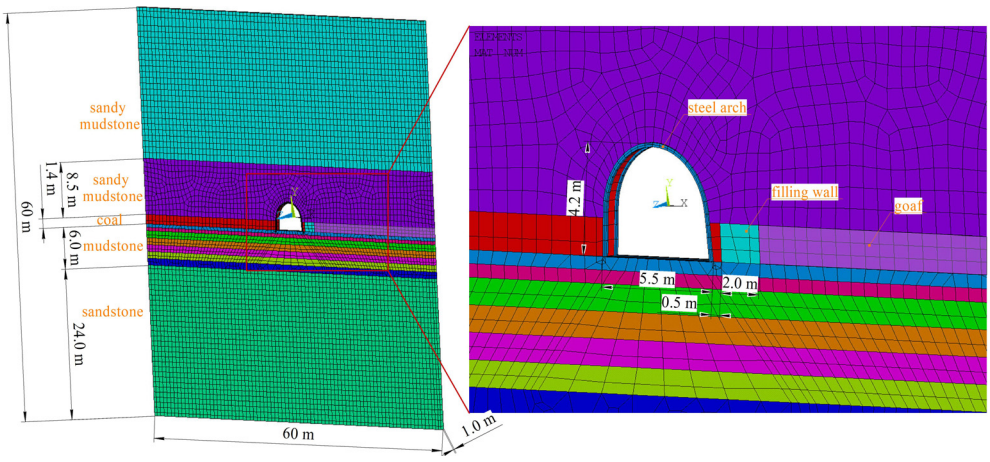

Fig. 3. Numerical simulation model.

Stress-strain state in surrounding rocks of gob-side entry retaining was simulated. Therefore, the parameters of intact rock were corrected to correspond to rock mass. The Hoek-Brown Criterion was used to calculate parameters of discontinuous surrounding rocks [42]. Hoek and Diederichs [43] empirical method was used to calculate the rock mass deformation modulus. The methodology for calculating parameters is presented in detail in the previous study [1]. The rock mass properties for studied strata are shown in Table 1. The failure criteria for strain was adopted in the range of "-0.03"–"+0.03", according to the laboratory tests of mudstone, siltstone, argillite [1]. Mechanical parameters of U-shaped steel support and filling wall are shown in Table 2.

Table 1. Intact rock properties and calculated rock mass properties.

Rock Strata	Intact rock			GSI/D/ m_i	Rock mass		
	Density, (kg/m^3)	Deformation modulus, (MPa)	Compressive strength, (MPa)		Deformation modulus, (MPa)	Compressive strength, (MPa)	Cohesion, (MPa)/ Internal friction angle, (deg)
Sandy mudstone	2400	7100	44.0	52/0.5/8	1191	1.76	2.83/24
Sandy mudstone	2400	5800	37.0	52/0.5/8	973	1.47	2.45/27
Coal seam	1300	1970	13.0	35/0/17	224	0.32	1.13/20
Mudstone	2300	4100	31.0	47/0.5/8	496	0.87	1.61/22
Sandstone	2400	8900	59.0	55/0.5/12	1804	2.89	3.9/34

The simulation was carried out step by step. The stress-strain state around the gateroad without floor support was studied at the first step (scheme 1). At the second step, the immediate floor was supported with rock bolts (scheme 2). The diameter of the corner rock bolts (which were bent) varied from 32 to 96 mm. At the third step, the near contour part of

these bolts was replaced with piles (scheme 3). The experimental design is shown in Fig. 4 and in table. 3.

Table 2. Steel arch frame and filling wall parameters for numerical simulation.

Compressive strength, (MPa)	Tensile strength, (MPa)	Deformation modulus, (GPa)	Poisson's ratio	Cohesion value, (MPa)	Angle of internal friction, (deg)
U-shaped steel arch frame					
295	295	200	0.27	–	–
Filling wall body					
3.62	0.16	1.48	0.3	3.33	29

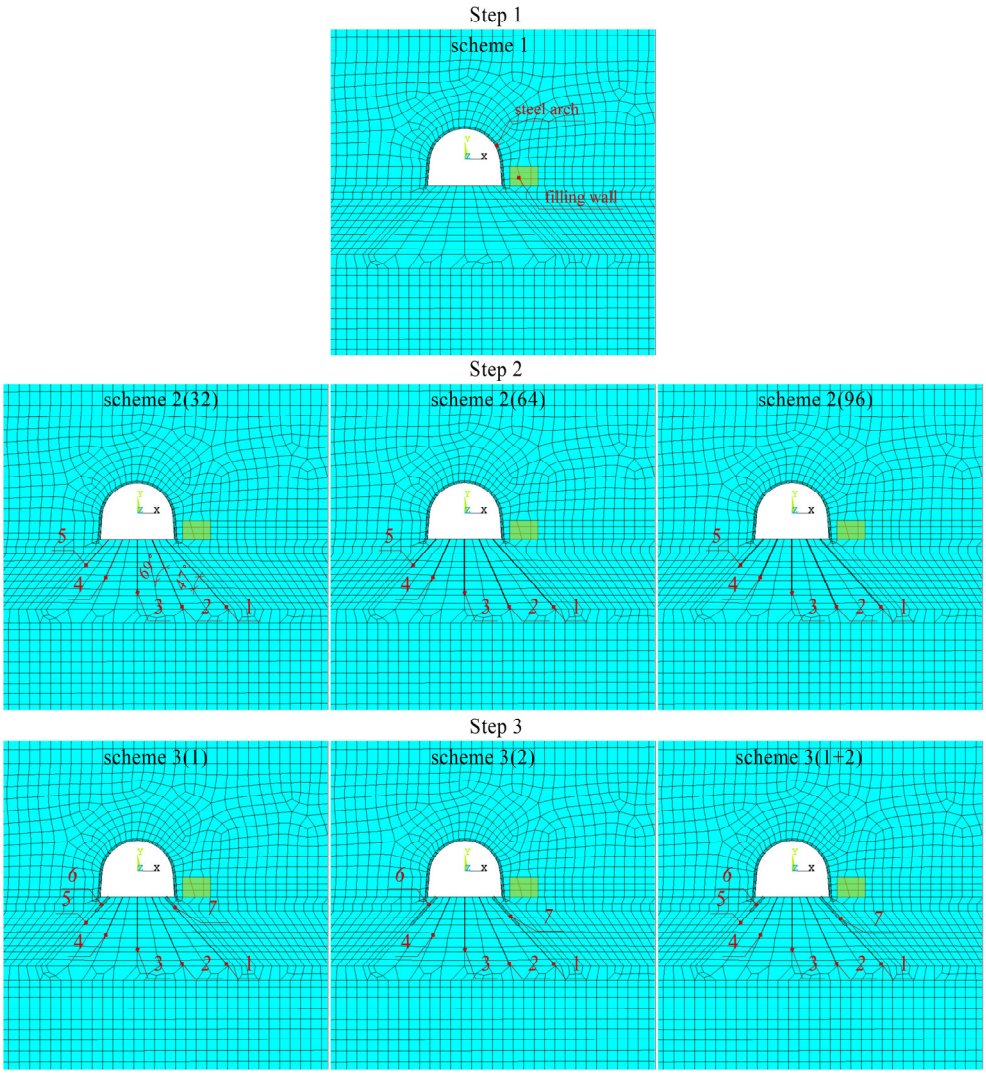

Fig. 4. Floor heave support schemes for numerical simulation: 1, 2, 3, 4, 5 – rock bolts; 6, 7 – steel piles.

Table 3. The parameters of floor heave control schemes.

Scheme	Number of rock bolts	Bolts length, (m)/diameter, (mm)					Piles length, (m)	
		Bolt No. 1	Bolt No. 2	Bolt No. 3	Bolt No. 4	Bolt No. 5	Pile No. 6	Pile No. 7
1st simulation step								
scheme 1	–	–	–	–	–	–	–	–
2nd simulation step								
scheme 2(32)	5	5/32	5/32	4/32	3/32	2/32	–	–
scheme 2(64)	5	5/64	5/64	4/64	3/64	2/64	–	–
scheme 2(96)	5	5/96	5/96	4/96	3/96	2/96	–	–
3rd simulation step								
scheme 3(1)	5	4/32	5/32	4/32	3/32	1/32	1	1
scheme 3(2)	4	3/32	5/32	4/32	3/32	-	2	2
scheme 3(1+2)	5	3/32	5/32	4/32	3/32	1/32	1	2

4 Results

4.1 First simulation step

The stress-strain cloud diagrams in the surrounding rocks are shown in Figs. 5 and 6. Analysis of the vertical stress distribution shows that the stress field is asymmetrical to the axis of the gateroad. It is clear since the geomechanical conditions in the surrounding rocks on the right and left sides of the gateroad are different. On the left side is a coal seam, and on the right side are a filling wall and goaf.

a *b*

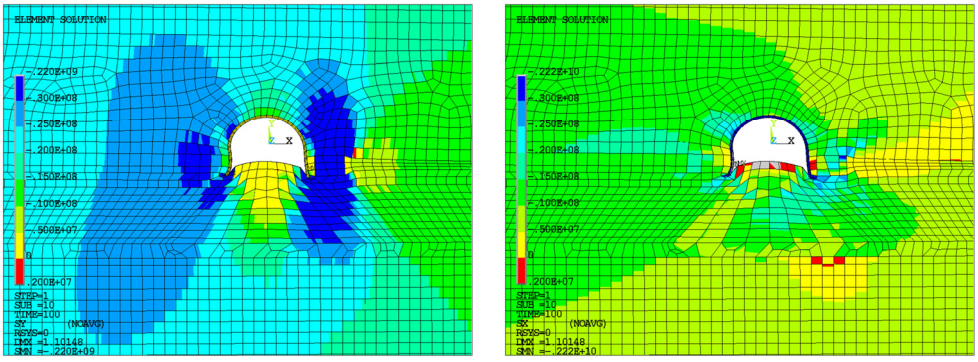

Fig. 5. Stress clouds around the gob-side entry retaining: (a) vertical stress; (b) horizontal stress.

To the left of the gateroad, the zone of maximum vertical stress is located at 1.6 – 3.0 m from the entry contour; the near-contour rocks are relieved (Fig. 5a). At the distance of 0-1.6 m from the gateroad sidewalls, the rocks are in the post-peak strain zones, as can be

seen in Fig. 6b, where the area of post-peak horizontal strains is highlighted in gray color on the left side of the entry.

a *b*

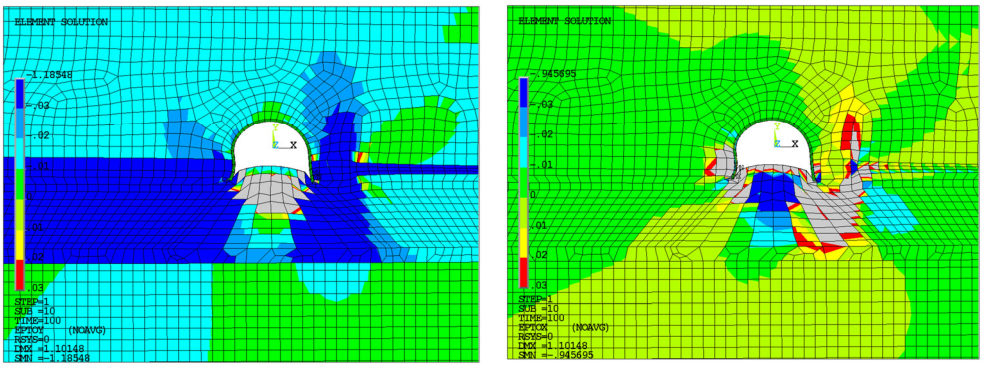

Fig. 6. Stress clouds around the gob-side entry retaining: (a) vertical stress; (b) horizontal stress.

Thus, in the left side of the gateroad, high vertical stresses are transmitted to the immediate floor at 1.6 – 3.0 m from the sidewall entry contour. On the right side of entry, the zone of high vertical stress has significantly larger magnitude. This is caused by the pressure of the main roof, which bend under the influence of gravity into the goaf and leaned on the filling wall. The filling wall undergoes high vertical stress and transmits it into the immediate floor. Thus, a zone of high vertical stress and strain is formed under the filling wall body (Fig. 5b and Fig. 6b). Stresses that arise in the immediate floor underneath the filling wall and coal seam exceed the tensile strength of intact rock in floor. This provokes dilatancy destruction of rocks and their expansion with displacement in the direction of the gateroad space. As a result, a zone of compressive horizontal strains, that highlighted in dark blue in Fig. 6b, appears under the gateroad span. Rocks compressed by high horizontal stresses tend to relief and displacement towards the gateroad space. This causes floor heave and post-peak vertical strain. The zone of post-peak vertical strain is highlighted in gray in Fig. 6a. The rocks in entry floor are stress relieved, as shown in Fig. 5b.

Thus, the cause of the floor uplift is the vertical expansion of rocks under the gateroad span. This expansion is a result of horizontal compression of rock. This compression is caused by the horizontal expansion of rocks in the floor underneath the U-shaped support legs and under the filling wall (Fig. 6b). Delamination of rocks in the indicated zones can be counteracted by rock bolts installation. The rock bolts length can be determined based on an analysis of the shape and size of the post-peak tensile strain zone. These zones are highlighted in gray in Fig. 6a and Fig. 6b.

4.2 Second simulation step

According to the floor support schemes of the 2nd simulation step, rock bolts were installed in the gateroad floor. In model the length of the bolts was greater than the size of the post-peak strain zone highlighted in gray in Fig. 6a and Fig. 6b. Since the mentioned zone is asymmetrical, the length of the bolts was also different (Table 3). Strain cloud diagrams in the surrounding rocks with different rock bolt diameters are shown in Fig. 7 and Fig. 8.

An analysis of the simulation results of scheme 2 (32) (Fig. 7a) shows that underneath the filling wall (near bolt No. 1), and underneath left arch frame leg (near bolt No. 5) zones of horizontal post-peak strains still appear as in scheme 1 (Fig. 6b). In this case, bolt No. 1

and bolt No. 5 critically bend in the near-contour area. To counteract the formation of a post-peak strains zone, was proposed to increase the diameter of bolt No. 1 and bolt No. 5. During the numerical experiment, the diameter of corner bolts varied from 32 mm to 96 mm. However, with a bolt diameter of 96mm in near-contour area, bolt No. 1 and bolt No. 5 are still bent (Fig. 7c).

An analysis of the vertical strain distribution results shows that an increase in the bolt diameter leads to a decrease in the vertical post-peak strain zone under central part of entry span (Fig. 8). With a bolt diameter of 96mm, a vertical post-peak strain zone under the central part of entry span is not formed. However, post-peak vertical strains still occur at the corners of the gateroad span.

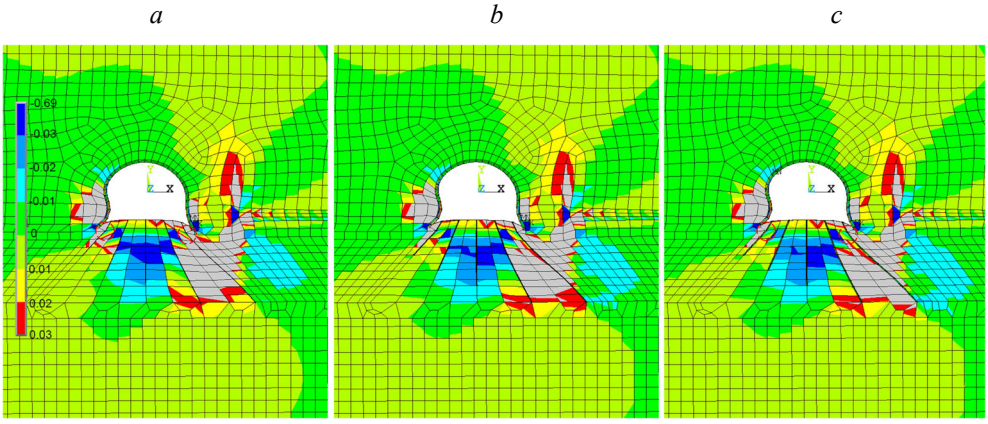

Fig. 7. Horizontal strain clouds around the gob-side entry retaining: (a) scheme 2(32); (b) scheme 2(64); (c) scheme 2(96).

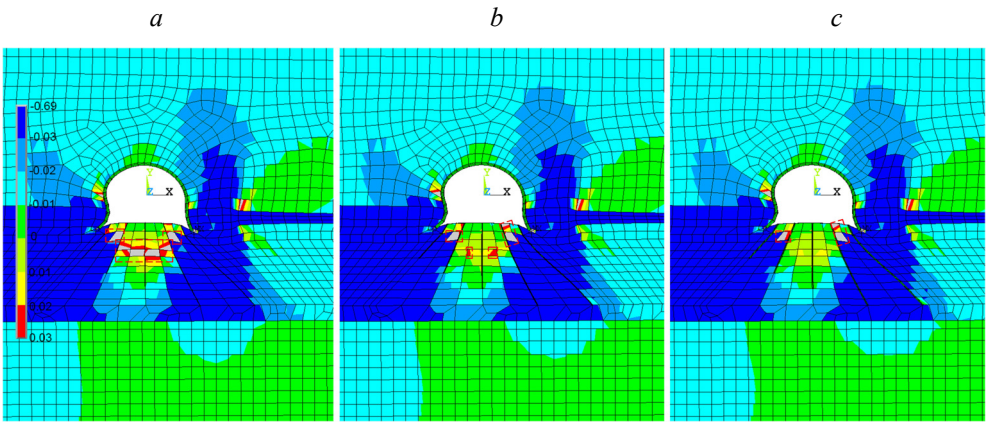

Fig. 8. Vertical strain clouds around the gob-side entry retaining: (a) scheme 2(32); (b) scheme 2(64); (c) scheme 2(96).

The reinforcement effect of rock bolts with different diameters on the floor uplift is clearly seen in the graphs of Fig. 9.

According to the floor heave analysis, can be concluded that the rock bolts reduce floor uplift by 2.9 – 3.6 times. So, after floor reinforcement with a bolt diameter of 32 mm, the maximum floor heave is 321 mm, that is 2.94 times less than the floor heave without reinforcement; with a bolt diameter of 96 mm, the floor uplift is 259 mm, that is 3.6 times

less than without floor support. As a result of analysis of the simulation results, it was found that the right leg of the support frame (from the side of the filling wall) is pressed into the immediate floor. The magnitude of this indentation at the first simulation step is 104 mm, at the second step – 165 mm. This means that the vertical convergence decreases on the mentioned indentation magnitude, i.e. the visible floor heave increases. The phenomenon of support frame leg indentation is called “false heaving” (the term was introduced by G. Litvinsky [44]). In-situ monitoring has repeatedly confirmed “false heaving”, as noted, for example, in previous study [45].

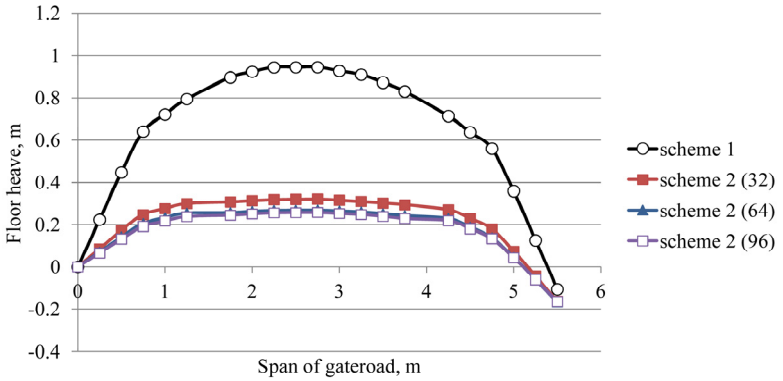

Fig. 9. The gateroad floor heave at first and second simulation steps.

The results obtained by numerical simulation may have errors for obvious reasons. However, considering that the floor uplift in the model without reinforcement differs from measured in-situ by 9.1%, can be assumed that the numerical model has sufficient accuracy. So, in-situ the floor heave (taking into account the indentation of the support frame legs) is 1150 mm, and in the model, it is 1048 mm. This is the basis for confidence in the obtained simulation results.

To prevent bending of the rock bolts in the near contour gateroad area and increase the reliability of floor reinforcement, at the next simulation step the near contour part of the bolts was replaced with piles.

4.3 Third simulation step

The support schemes of the 3rd simulation step were a modification of the 2nd step schemes, in which the corner rock bolts were partially replaced by piles. The diameter of rock bolts at 3rd step was 32 mm. The support scheme design is shown in Fig. 4. Fig. 10 and Fig. 11 show strain cloud diagrams in the surrounding rocks with different floor reinforcement schemes.

Piles installation reduces the zone of tensile horizontal post-peak strains in the right corner of the gateroad span and compressive post-peak strains underneath the central part of the gateroad span (Fig. 10). Vertical post-peak strains after piles installation do not occur either in the center of the gateroad span or in its corners (Fig. 11). The stress-strain state in the entry floor after the piles installation is more favorable than after the rock bolting. Scheme 3(2) gives the best reinforcing effect of the compared schemes. However, there is no significant difference between scheme 3(2) and scheme 3(1+2). The same conclusion can be drawn from an analysis of the floor heave magnitudes (Fig. 12). Schemes that are studied at the third simulation step show the same effectiveness in counteracting floor uplift. Moreover, after piles installation, the indentation of the support leg in immediate floor on the right side of the gateroad is less than in the cases of rock bolting.

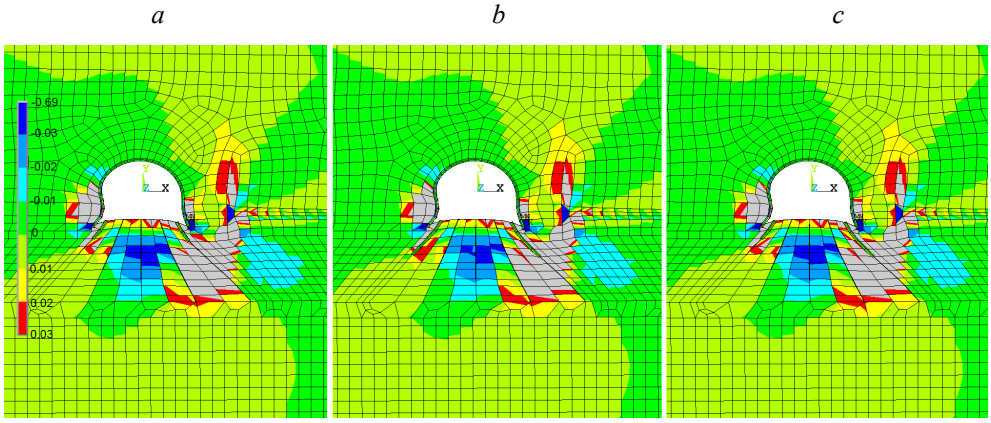

Fig. 10. Horizontal strain clouds around the gob-side entry retaining: (a) scheme 3(1); (b) scheme 3(2); (c) scheme 3(1+2).

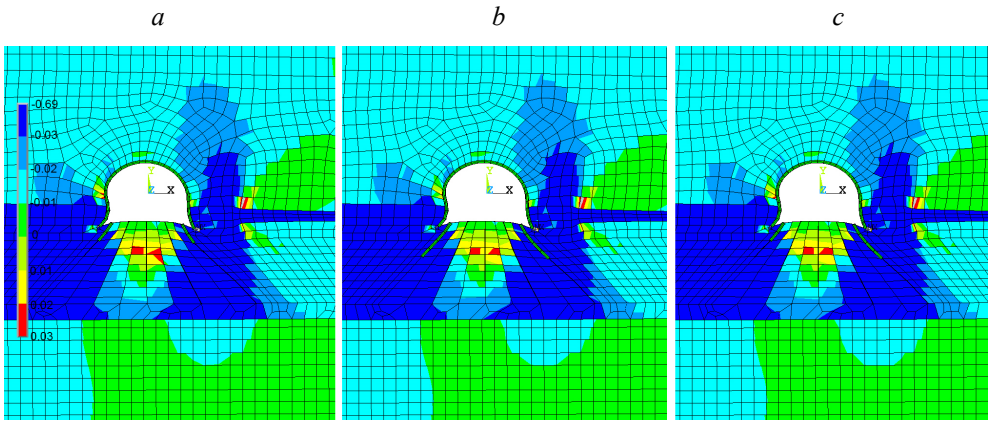

Fig. 11. Vertical strain clouds around the gob-side entry retaining: (a) scheme 3(1); (b) scheme 3(2); (c) scheme 3(1+2).

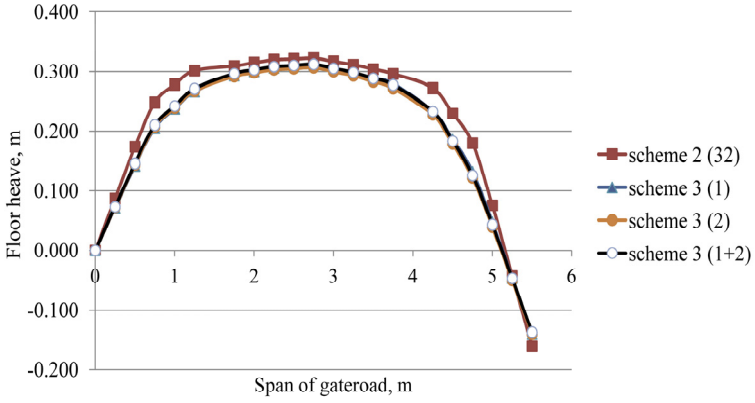

Fig. 12. The gateroad floor heave at second and third simulation steps.

In the center part of the entry span, the floor uplift with scheme 3(2) and scheme 3(1+2) is 4% and 6% less than with scheme 2(32) respectively. At 1.25 m from the gateroad sidewall

contour, the floor uplift with scheme 3(2) and scheme 3(1+2) is 15% and 25% less than with scheme 2(32) respectively. In this case, the right pile still bends in the near contour area, while the left one saves its form.

5 Discussion

Several conclusions can be drawn according to the above analyses:

(1) The surrounding rock of gob-side entry is in asymmetrical strain-stress field. The reason for this is bending of the main roof into the goaf behind the longwall face. Stress redistribution in surrounding rocks leads to high vertical stress in the sides of the gateroad. The filling wall, which is the support for the main roof, transmits vertical stresses into the immediate floor, which provokes dilatancy destruction of rocks and their displacement towards the gateroad space. At the same time, zones of post-peak strains appear in the floor, the shape and size of which indicate a zone of potential reinforcing.

(2) Choosing a rock bolt scheme, it is advisable to take the length of the bolts larger than the size of the post-peak strain zone. With this approach, according to the simulation results, rock bolts with a diameter of 32 mm can reduce the floor heave by 2.94 times after installation according to scheme 2(32). The increase of the bolts diameter significantly reduces the size of the post-peak strain zone in the gateroad floor and reduces floor uplift. So, with a bolt diameter of 96 mm, the floor heave decreases by 3.6 times, and vertical post-peak strains underneath the central part of the gateroad span do not occur. However, bolts of this diameter are, in fact, small piles. It is difficult to imagine their practical implementation. These bolts require the development of special installation technology and equipment for borehole drilling. Their implementation will lead to increased cost of bolts, labor costs and transportation costs. However, from a theoretical perspective, the obtained results show that the load-bearing capacity of bolts is an important factor that contributes on the floor heave mechanism.

A similar effect can also be achieved by increasing the rock bolts amount. For example, the load-bearing capacity of 1 rock bolt with a diameter of 96 mm is equivalent to the load-bearing capacity of 9 rock bolts with a diameter of 32 mm. However, an increase of the metal intensity of the support system is not an effective way to gateroad stability control. A promising way, according to the authors, is the implementation of rock bolts with increased load-bearing capacity, for example energy-absorbing bolts [46 48]. The effectiveness of floor heave control can be increased by new rock bolt designs. This confirms the prospect of developing an energy-absorbing bolts, including non-metallic ones. However, this approach is not considered in this paper, but is one of the directions for further research.

(3) The modification of the traditional rock bolt reinforcement scheme with a bolt diameter of 32 mm is offered by the additional installation of piles in the gateroad corners along the rock bolt axis. Such piles installation reduces the zone of horizontal post-peak strains. Vertical post-peak strains do not occur in the entry floor after the installation of piles. At the same time, the floor uplift is slightly less than after reinforcement by rock bolts with a diameter of 32 mm. The simulation results show that the optimal variant is a floor support scheme with two piles, 1 m and 2 m long (scheme 3(1+2)). With this scheme, floor uplift decreases by 3.05 times, and post-peak tensile strains do not appear in the immediate floor. The post-peak strain zones do not appear so it can be concluded that the reinforcement scheme has a sufficient margin of reliability and the floor rocks retain their bearing capacity.

The implementation of the proposed scheme requires a more complex technology for floor support. The traditional full resin bolts with a diameter of 32 mm and steel pile with the design, described in the studies [38, 39], were proposed. The main recommendations are as follows. Rock bolts and piles have to be installed outside the front abutment pressure of

longwall face. Boreholes for rock bolts in the gateroad floor are drilled according to a template that corresponds to scheme 3(1+2). In the entry corners, holes for piles are drilled by mine drilling machine, for example SBM 1. At the same time, pile boreholes are drilled along the bolts borehole axis, expanding it to a diameter of 219 mm. First of all, corner full resin bolts are installed through the pile borehole; their rock bolt plates are located at the bottom of the pile boreholes. After this, metal tubes are installed in the pile boreholes and filled with concrete. Fig. 13 shows the proposed design of support scheme.

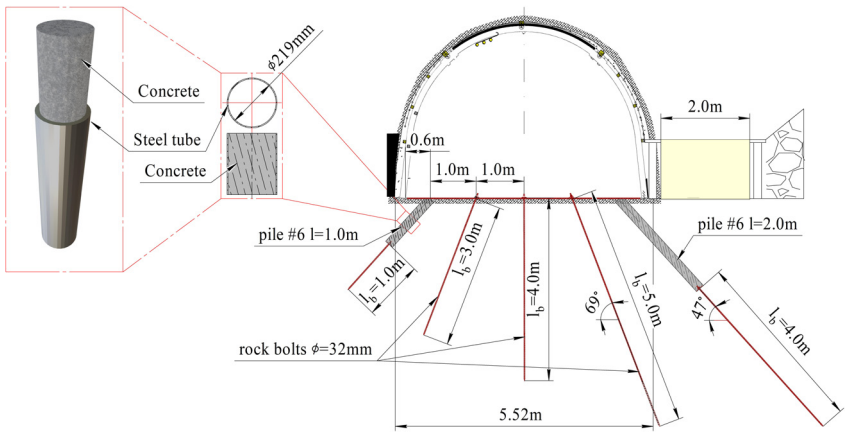

Fig. 13. Design of proposed support scheme (scheme 3(1+2)).

A comparison of the materials costs after implementation of the proposed floor support scheme and rock bolt reinforcement schemes is shown in Table 4.

Table 4. The parameters of floor heave control schemes.

Scheme	Summary rock bolts length, m	Summary piles length, m	Cost of bolts, Euro	Cost of polyester resin capsule, Euro	Cost of tube, Euro	Cost of concrete, Euro	Total cost, Euro
scheme 2(32)	20	–	114.77	32.00	–	–	146.77
scheme 2(64)	20	–	459.08	128.00	–	–	587.08
scheme 2(96)	20	–	1032.93	288.00	–	–	1320.93
scheme 3(1+2)	17	3	97.55	27.20	87.60	7.01	219.36

The traditional floor support scheme with rock bolts with a diameter of 32 mm is the low-cost variant among compared ones. The material cost of the one row of bolts with scheme 2(32) is 146.77 Euro. The increase of the rock bolt diameter leads to an increase in material cost, disproportionate to the effect. For example, doubling of the rock bolts diameter leads to a reduction in floor uplift by 15% and an increase in materials cost by 4 times. At the same time, the stress distribution in the gateroad floor does not differ significantly, and zones of post-peak strains still appear in the immediate floor. Additional installation of corner piles with scheme 3(1+2) leads to the change of the stress-strain field in the immediate floor. In this variant, post-peak strain zones do not appear in the gateroad

floor. At the same time, material costs in proposed scheme increase by 49%, and floor uplift decreases by 4%.

According to the authors of this paper, the proposed in previous studies [38, 39] steel pile design is not the best. Optimization of piles design to reduce their cost requires additional research and is not studied in this paper. In the materials cost structure of scheme 3(1+2), 40% of total cost is the cost of the tubes. Applying of worn elements of suppression system pipeline as tubes for piles will make this scheme more economical. The modification of the design of tubes and rock bolts with increased load-bearing capacity is the prospect object for future research.

6 Conclusions

This study was focused on the prospective ways of floor heave control in gob-side entry retaining. Floor heave control with rock bolts reinforcement was studied. The base of study was numerical simulation of stress-strain state of surrounding rock by ANSYS code. In the result, a modified floor heave control method based on rock bolt reinforcement was proposed. Analysis of the simulation results shows that the main prospects for further research of floor heave control methods are in improving the design of rock bolts in order to increase their load-bearing capacity and in improving the design of piles in order to reduce their cost. This will be further studied by the authors.

The authors are aware that numerical simulation results are valid only for mechanical parameters of rock mass, filling wall, support elements, that were modeled, and overburden stress at the depth of 900 m. However, the mechanism of floor heave and effectiveness of floor heave control technology, that were studied, will obviously not change significantly in similar geological conditions.

References

1. Sakhno, I., & Sakhno, S. (2023). Numerical studies of floor heave control in deep mining roadways with soft rocks by the rock bolts reinforcement technology. *Advances in Civil Engineering*, *2023*, 1-23. https://doi.org/10.1155/2023/2756105
2. Qi, F., Ma, Z., Yang, D., Li, N., Li, B., Wang, Z., & Ma, W. (2021). Stability control mechanism of high-stress roadway surrounding rock by roof fracturing and rock mass filling. *Advances in Civil Engineering*, *2021*, 1-17. https://doi.org/10.1155/2021/6658317
3. Wang, Q., Jiang, B., Pan, R., Li, S.C., He, M.C., Sun, H.B., Qin, Q., Yu, H.C., & Luan, Y.C. (2018). Failure mechanism of surrounding rock with high stress and confined concrete support system. *International Journal of Rock Mechanics and Mining Sciences*, (102), 89-100. https://doi.org/10.1016/j.ijrmms.2018.01.020
4. He, M., Gao, Y., Yang, J., Wang, J., Wang, Y., & Zhu, Z. (2018). Engineering experimentation of gob-side entry retaining formed by roof cutting and pressure release in a thick-seam fast-extracted mining face. *Rock and Soil Mechanics*, (39), 254-264.
5. Yuan, L. (2016). Control of coal and gas outbursts in Huainan mines in China: A review. *Journal of Rock Mechanics and Geotechnical Engineering*, *8*(4), 559-567. https://doi.org/10.1016/j.jrmge.2016.01.005
6. Ning, J., Wang, J., Bu, T., Hu, S., & Liu, X. (2017). An innovative support structure for gob-side entry retention in steep coal seam mining. *Minerals*, *7*(5), 75. https://doi.org/10.3390/min7050075
7. Gong, P., Ma, Z., Ni, X., & Zhang, R.R. (2017). Floor heave mechanism of gob-side entry retaining with fully-mechanized backfilling mining. *Energies*, (10), 2085. http://doi:10.3390/en10122085

8. Li, Z., Zhang, Y., Ma, Q., Zheng, Y., Song, G., Yan, W., Zhang, Y., & Hu, L. (2023). The floor heave mechanism and control technology of gob-side entry retaining of soft rock floor. *Sustainability*, *15*(7), 6074. https://doi.org/10.3390/su15076074
9. Yu, G., Wang, J., Hu, J., Zhu, D., Sun, H., Ma, X., Ming. W., & Li W. (2021). Innovative control technique for the floor heave in goaf-side entry retaining based on pressure relief by roof cutting. *Mathematical Problems in Engineering*, *2021*, 1-17. https://doi.org/10.1155/2021/7163598
10. Faria Santos, C., & Bieniawski, Z.T. (1989). Floor design in underground coal mines. *Rock Mechanics and Rock Engineering*, *22*(4), 249-271. https://doi.org/10.1007/bf01262282
11. Mo, S., Ramandi, H.L., & Oh, J. (2018). A Review of Floor Heave Mechanisms in Underground Coal Mine Roadways. In *The Fourth Australasian Ground Control in Mining Conference* (pp. 196-206). Sydney, New South Wales, Australia: The Australasian Institute of Mining and Metallurgy.
12. Mo, S., Ramandi, H.L., Oh, J., Masoumi, H., Canbulat, I., Hebblewhite, B., & Saydam, S. (2020). A new coal mine floor rating system and itsapplication to assess the potential of floor heave. *International Journal of Rock Mechanics and Mining Sciences*, (128), 104241. https://doi.org/10.1016/j.ijrmms.2020.104241
13. Sakhno, I., Liashok, Ia., Sakhno, S., & Isaienkov, O. (2022). Method for controlling the floor heave in mine roadways of underground coal mines. *Mining of Mineral Deposits*, *16*(4), 1-10. https://doi.org/10.33271/mining16.04.001
14. Babets, D., Sdvyzhkova, O., Hapieiev, S., Shashenko, O., & Prykhodchenko, V. (2023). Multifactorial analysis of a gateroad stability at goaf interface during longwall coal mining – A case study. *Mining of Mineral Deposits*, *17*(2), 9-19. https://doi.org/10.33271/mining17.02.009
15. Cicek, S., Tulu, I.B., Van Dyke, M., Klemetti, T., & Wickline, J. (2020). Application of the coal mine floor rating (CMFR) to assess the floor stability in a Central Appalachian Coal Mine. *International Journal of Mining Science and Technology*, *31*(1), 83-89. https://doi.org/10.1016/j.ijmst.2020.12.022
16. Sakhno, I., Sakhno, S., Skyrda, A., & Popova, O. (2022). Numerical modeling of controlling a floor heave of coal mine roadways with a method of reinforcing in wet soft rock. *Geofluids*, *2022*, 1-14. https://doi.org/10.1155/2022/3855799
17. Małkowski, P., Ostrowski, Ł., & Stasica, J. (2022). Modeling of floor heave in underground roadways in dry and waterlogged conditions. *Energies*, *15*(12), 4340. https://doi.org/10.3390/en15124340
18. Chang, Z., Yan, C., Xie, W., Lu, Z., Lan, H., & Mei, H. (2024). Large-scale field tunnel model experience and time-dependent floor heave induced by humidification. *Tunnelling and Underground Space Technology*, (145), 105615. https://doi.org/10.1016/j.tust.2024.105615
19. Yue, J., Liang, Q., Zhang, T., & Fan, C. (2024). Research on mechanical response and time-space distribution of supporting structure of deep-buried tunnel in naturally water-rich loess, *Tunnelling and Underground Space Technology*, (147), 105688, https://doi.org/10.1016/j.tust.2024.105688
20. Zhang, Z., Sun, J., Ma, Y., Wang, Q., Li, H., & Wang, E. (2024). Research on the Influence Mechanism of Moisture Content on Macroscopic Mechanical Response and Microscopic Evolution Characteristic of Limestone. *Buildings*, *14*(2), 469. https://doi.org/10.3390/buildings14020469
21. Chen, Y., Li, Q., Pu, H., Wu, P., Chen, L., Qian, D., Shi, X., Zhang, K. & Mao, X. (2020). Modeling and simulation of deformation mechanism of soft rock roadway considering the mine water. *Geofluids*, *2020*, 1-22. https://doi.org/10.1155/2020/8812470
22. Dychkovskyi, R., Tabachenko, M., Zhadiaieva, K., Dyczko, A., & Cabana, E. (2021). Gas hydrates technologies in the joint concept of geoenergy usage. *E3S Web of Conferences*, (230), 01023. https://doi.org/10.1051/e3sconf/202123001023
23. Kononenko, M., Khomanko, O., Cabana, E., Mirek A., Dyczko A., Prostański, D. & Dychkovskyi R. (2023) Using the methods to calculate parameters of drilling and + blasting operations for emulsion explosives. *Acta Montanistica Slovaca*, *28*(3), 655-667. https://doi.org/10.46544/ams.v28i3.10

24. Dyczko, A. (2023). Real-time forecasting of key coking coal quality parameters using neural networks and artificial intelligence. *Rudarsko-Geološko-Naftni Zbornik*, *38*(3), 105-117. https://doi.org/10.17794/rgn.2023.3.9
25. Kononenko, M., Khomenko, O., Sadovenko, I., Sobolev, V., Pazynich, Y., & Smoliński, A. (2023). Managing the rock mass destruction under the explosion. *Journal of Sustainable Mining*, *22*(3), 240. https://doi.org/10.46873/2300-3960.1391
26. Xie, S., Li, H., Chen, D., Feng, S., Ma, X., Jiang, Z., & Cui, J. (2022). New technology of pressure relief control in soft coal roadways with deep, violent mining and large deformation: A Key Study. *Energies*, *15*(23), 9208. https://doi.org/10.3390/en15239208
27. Yang, T., & Zhang, J. (2021). Research on the treatment technology of soft rock floor heave based on a model of pressure-relief slots. *Arabian Journal of Geosciences*, *14*(13), 1278. https://doi.org/10.1007/s12517-021-07673-4
28. Guo, D., Kang, X., Lu Z., & Chen, Q. (2021). Mechanism and control of roadway floor rock burst induced by high horizontal stress. *Shock and Vibration.*, (5), 1-13. https://doi.org/10.1155/2021/6745930
29. Li, Z., Zhang, Y., Ma, Q., Zheng, Y., Song, G., Yan, W., Zhang, Y., & Hu, L. (2023). The Floor Heave Mechanism and Control Technology of Gob-Side Entry Retaining of Soft Rock Floor. *Sustainability*, *15*(7), 6074. https://doi.org/10.3390/su15076074
30. Lai, X., Xu, H., Shan, P., Kang, Y., Wang, Z., & Wu, X. (2020). Research on Mechanism and Control of Floor Heave of Mining-Influenced Roadway in Top Coal Caving Working Face. *Energies*, *13*(2), 381. https://doi.org/10.3390/en13020381
31. He, M.C., Zhang, G.F., Wang, G.L., Xu, Y.L., Wu, C.Z., & Tang, Q.D. (2009). Research on mechanism and application to floor heave control of deep gateway. *Chinese Journal of Mechanical Engineering*, (28), 2593-2598.
32. Yang, J., Zhou, K., Cheng, Y., Gao, Y., Wei, Q., & Hu, Y. (2019). Mechanism and control of roadway floor heave in the paleogene soft rock surroundings. *Geotechnical and Geological Engineering*, *37*(6), 5167-5185. https://doi.org/10.1007/s10706-019-00970-6
33. Shimada, H., Hamanaka, A., Sasaoka, T., & Matsui, K. (2014). Behaviour of grouting material used for floor reinforcement in underground mines. *International Journal of Mining, Reclamation and Environment*, *28*(2), 133-148. https://doi.org/10.1080/17480930.2013.804257
34. Zhang, Z.Y., & Shimada, H. (2018). Numerical study on the effectiveness of grouting reinforcement on the large heaving floor of the deep retained goaf-side gateroad: A case study in China. *Energies*, (11), 1001. https://doi.org/10.3390/en11041001
35. Zhai, X.X., Qin, L.T., & Chen, C.Y. (2017). Combined Supporting Technology of Anchoring and Grouting and Floor Relief in Deep Chamber of Belt Conveyor. *Chinese Journal of Underground Space and Engineering*, (5), 1363-1372.
36. Kang, X., Guo, D., & Lu, Z. (2021). Mechanism of roadway floor heave controlled by floor corner pile in deep roadway under high horizontal stress. *Advances in Civil Engineering*, *2021*, 1-10. https://doi.org/10.1155/2021/6669233
37. Polyanska, A., Pazynich, Y., Poplavska, Z., Kashchenko, Y., Psiuk, V., & Martynets, V. (2024). Conditions of Remote Work to Ensure Mobility in Project Activity. *Lecture Notes in Mechanical Engineering*, 151-166. https://doi.org/10.1007/978-3-031-56474-1_12
38. Xu, Y., Chen, J., & Bai, J. (2016). Control of floor heaves with steel pile ingob-side entry retaining. *International Journal of Mining Science and Technology*, *26*(3), 527-534. https://doi.org/10.1016/j.ijmst.2016.02.024
39. Zhu, B., Weifeng, K., Jiami, X., & Yanjun, S. (2016). Numerical simulation research of construction method for shallow buried large section tunnel. *The Open Civil Engineering Journal*, *10*(1), 578-597. https://doi.org/10.2174/1874149501610010578
40. Sakhno, I.G., Molodetskyi, A.V., & Sakhno, S.V. (2018). Identification of material parameters for numerical simulation of the behavior of rocks under true triaxial conditions. *Naukovyi Visnyk Hatsionalnoho Hirnychoho Universytetu*, (5), 48-53. https://doi.org/10.29202/nvngu/2018-5/4

41. Li, J., Huang, Y., Zhai, W., Li, Y., Ouyang, S., Gao, H., Li, W., Ma, K., & Wu, L. (2020) Experimental study on acoustic emission of confined compression of crushed gangue under different loading rates: Disposal of gangue solid waste. *Sustainability*, *12*(9), 3911. https://doi.org/10.3390/su12093911
42. Hoek, E., Carranza-Torres, C., & Corkum, B. (2002). Hoek-Brown failure criterion – 2002 edition. In *Proceedings of the 5th North American Rock Mechanics Symposium and the 17th Tunnelling Association of Canada Conference* (pp. 267-271). Toronto, Canada.
43. Hoek, E., & Diederichs, M. (2006). Empirical estimates of rock mass modulus. *International Journal of Rock Mechanics and Mining Sciences*, *43*(2), 203-215. https://doi.org/10.1016/j.ijrmms.2005.06.005
44. Sakhno, I., Isayenkov, O., & Rodzin, S. (2017). Local reinforcing of footing supported in the destroyed rock massif. *Mining of Mineral Deposits*, *11*(1), 9-16. https://doi.org/10.15407/mining11.01.009
45. Litvinsky, G.G., & Fesenko, E.V. (2010). Prognoz pucheniya porod pochvy gornykh vyrabotok – veroyatnostnyy aspekt. *Zbirnyk naukovykh prats DonDTU*, 4-13.
46. Li, C.C., Stjern, G. & Myrvang A. (2014). A review on the performance of conventional and energy-absorbing rockbolts. *Journal of Rock Mechanics and Geotechnical Engineering*, *6*(4), 315-327. https://doi.org/10.1016/j.jrmge.2013.12.008
47. He, M., Gong, W., Wang, J. Qi, P., Tao, Zh. Du, Sh., & Peng, Y. (2014). Development of a novel energy-absorbing bolt with extraordinarily large elongation and constant resistance. *Journal of Rock Mechanics and Mining Sciences*, *(*67), 29-42. https://doi.org/10.1016/j.ijrmms.2014.01.007
48. Sakhno, I., Sakhno, S., Isaienkov, O., & Kurdiumow, D. (2019). Laboratory studies of a high-strength roof bolting by means of self-extending mixtures. *Mining of Mineral Deposits*, *13*(2), 17-26. https://doi.org/10.33271/mining13.02.017